Kidney International, Vol. 60 (2001), pp. 106–116

Podocyte injury underlies the progression of focal segmental glomerulosclerosis in the *fa*/*fa* Zucker rat

Nikolaus Gassler, Marlies Elger, Bettina Kränzlin, Wilhelm Kriz, and Norbert Gretz, with the technical assistance of Brunhilde Hähnel, Hiltraud Hosser, and Inge Hartmann

Pathologisches Institut and Institut für Anatomie und Zellbiologie, Medizinische Fakultät Heidelberg, Universität Heidelberg, Heidelberg; and Zentrum für Medizinische Forschung, Medizinische Fakultät Mannheim, Universität Heidelberg, Mannheim, Germany

Podocyte injury underlies the progression of focal segmental glomerulosclerosis in the *fa*/*fa* Zucker rat.

Background. The progression of diabetic nephropathy to chronic renal failure is based on the progressive loss of viable nephrons. The manner in which nephrons degenerate in diabetic nephropathy and whether the injury could be transferred from nephron to nephron are insufficiently understood. We studied nephron degeneration in the *fa*/*fa* Zucker rat, which is considered to be a model for non-insulin-dependent diabetes mellitus.

Methods. Kidneys of *fa*/*fa* rats with an established decline of renal function and of *fa*/+ controls were structurally analyzed by advanced morphological techniques, including serial sectioning, high-resolution light microscopy, transmission electron microscopy, cytochemistry, and immunohistochemistry. In addition, tracer studies with ferritin were performed.

Results. The degenerative process started in the glomerulus with damage to podocytes, including foot process effacement, pseudocyst formation, and cytoplasmic accumulation of lysosomal granules and lipid droplets. The degeneration of the nephron followed the tuft adhesion-mediated pathway with misdirected filtration from capillaries included in the adhesion toward the interstitium. This was followed by the formation of paraglomerular spaces that extended around the entire glomerulus, as well as via the glomerulotubular junction, to the corresponding tubulointerstitium. This mechanism appeared to play a major role in the progression of the segmental glomerular injury to global sclerosis as well as to the degeneration of the corresponding tubule.

Conclusions. The way a nephron undergoes degeneration in this process assures that the destructive effects remain confined to the initially affected nephron. No evidence for a transfer of the disease from nephron to nephron at the level of the tubulointerstitium was found. Thus, each nephron entering this pathway to degeneration appears to start separately with the same initial injuries at the glomerulus.

Key words: nephron degeneration, diabetic nephropathy, non-insulin–dependent diabetes mellitus, progressive renal disease, glomerular injury.

Received for publication September 28, 2000
and in revised form January 22, 2001
Accepted for publication January 25, 2001

The *fa*/*fa* Zucker rat is generally considered to be a rat model for non-insulin–dependent diabetes mellitus (NIDDM) [1, 2]. The *fa* gene was first described in the obese Zucker rat, and it has been backcrossed into a number of strains that exhibit a moderate degree of hyperglycemia. A partially inbred strain, the Zucker diabetic fatty rat (*fa*/*fa* rat)—due to its marked insulin resistance—has been frequently used in experimental studies addressing specific questions in NIDDM, obesity, and hypertension [1–4].

Obese Zucker *fa*/*fa* rats are pathophysiologically characterized by hyperphagia, obesity, hyperlipidemia, peripheral insulin resistance, hyperinsulinemia, and impaired glucose tolerance [3, 5–8]. In these rats, an autosomal recessive mutation of the *fa* gene, encoding the leptin receptor, is found [7]. Male *fa*/*fa* rats exhibit most of the metabolic abnormalities associated with human type II diabetes [9].

The *fa*/*fa* rat strain has been employed to gain more insight into the pathogenesis of the nephropathy associated with type II diabetes mellitus [10–14]. Proteinuria, focal segmental glomerulosclerosis (FSGS), and tubulointerstitial injury, ultimately leading to renal failure, are regularly seen in *fa*/*fa* rats with increasing age [5, 11]. A recent study presents convincing evidence that the disease starts with podocyte injury and that the role of the mesangium in disease development is marginal, at best [9].

The present study addresses two main questions. First, how (not primarily why) do nephrons develop glomerulosclerosis and nephron degeneration in the *fa*/*fa* Zucker rat? Is it appropriate to consider the renal injury of this rat as a model for the nephropathy encountered in type II diabetes in humans? Second, what are the mechanisms

underlying disease progression? Progression of chronic renal disease is based on the progressive loss of viable nephrons. Thus, is there a mechanism by which the disease, once it has started, jumps from nephron to nephron, or is each nephron separately affected by the same glomerular or systemic factors? The present study provides strong evidence that there is not a nephron to nephron transfer of the disease. This conclusion appears to be of more general relevance with respect to progressive renal disease, and is not just valid for the *fa*/*fa* Zucker rat.

METHODS

Animal breeding and clinical investigations

Analyses were performed in 11 male obese *fa*/*fa* Zucker rats and 4 lean *fa*/+ Zucker rats (Harlan, Borchen, Germany) serving as controls. The animals were approximately 10 months old. They were fed a standard rat chow containing 19% protein and 3.3% fat (Ssniff, Soest, Germany) and had free access to tap water. Urinary protein (Coomassie Blue) and albumin (ICN Biomedicals GmbH, Eschwege, Germany) excretion were determined in animals in metabolic cages after a 24-hour fasting period. Immediately thereafter, the animals were anesthetized with ketamine and xylazine, and blood samples were taken to determine urea, glucose, cholesterol, and triglycerides (Hitachi 704 Automatic Analyzer; Boehringer Mannheim, Mannheim, Germany). Finally, the animals were subjected to perfusion fixation (discussed later in this article).

Processing kidneys for morphological and immunohistochemical evaluation

For the structural and immunohistochemical investigations, kidneys were fixed by total body perfusion after anesthesia, as described previously [15]. Briefly, the abdominal cavity was opened, and the kidneys were retrogradely perfused via the abdominal aorta without prior flushing of the vasculature using a perfusion pressure of 220 mm Hg for two minutes. The fixative contained 2% paraformaldehyde in phosphate-buffered saline (PBS; pH 7.4).

For immunohistochemistry, tissue blocks of right kidneys, immediately after the end of the perfusion, were shock frozen in melting isopentane cooled by liquid nitrogen and stored at –70°C until use. In addition, specimens of the right kidneys were embedded in Paraplast.

For high-resolution light microscopy (HRLM) and transmission electron microscopy (TEM), tissue of the left kidneys was postfixed overnight with 2% glutaraldehyde in 0.1 mol/L PBS at 4°C. The specimens were further fixed by 1% OsO_4, dehydrated in a graded series of ethanols, and embedded in Epon 812.

Epon blocks were sectioned with an Ultracut E microtome (Reichert-Jung, Vienna, Austria). A series of 1 μm sections was used to establish the kind of damage in individual nephrons. Each section in the series was cut with an appropriate diamond knife, stained with azur II and methylene blue according to Richardson, Jarett, and Finke [16], and was observed in a Polyvar 2 light microscope (Reichert-Jung). For TEM, ultrathin sections (70 nm) were stained with uranyl acetate and subsequently with Reynolds lead citrate, and were finally examined in a Philips EM 301 transmission electron microscope (Philips Electronics, Eindhoven, The Netherlands).

Morphometrical analysis and damage index

Thickness of the glomerular basement membrane (GBM) was evaluated in five randomly selected *fa*/*fa* rats and 4 *fa*/+ controls using the method of Jensen, Gundersen, and Osterby [17]. Briefly, photographs of six randomly selected different positions of the glomerular basements membrane in four glomeruli per animal were prepared with a final magnification of ×36,000. Using a set of test lines, the membrane thickness was evaluated with a computer assisted program (ViDS IV semi automatic image analysis system; AMS, Cambridge, UK).

In addition, a glomerular damage score was established for each *fa*/*fa* animal ($N = 9$) and the *fa*/+ controls ($N = 4$). Per animal, all glomerular profiles found in sections from five randomly selected epon blocks were evaluated (that is, 183 to 236 glomeruli per animal). Each glomerular profile was graded and assigned to one of three groups with respect to the degree of glomerular damage. Glomerular profiles with cytoplasmic droplets in podocytes and/or pseudocysts were assigned to group 1 (early changes); group 2 (moderate changes) consisted of glomerular profiles that in addition to group 1 lesions exhibited capillary ballooning in at least three capillary loops; glomerular profiles with tuft adhesion, synechia, or global sclerosis were collected in group 3 (advanced lesions). To calculate a score, group 1 lesions were factored with one, group 2 with two, and group 3 with three, and the values were added up. In addition, the group 3 changes were separately considered as a percentage of sclerotic glomeruli. Data were statistically analyzed for correlation using the SPSS analysis program (Chicago, IL, USA).

Antibodies and immunohistochemistry

Anti-rat collagen types I (diluted 1:10) and IV (1:30) polyclonal antibodies both raised in rabbit (Sanbio, Uden, The Netherlands) as well as Cy 2-labeled anti-rabbit IgG raised in goat (1:200; Dianova, Hamburg, Germany) were used.

For immunohistochemical procedures, representative paraffin-embedded serial sections (each section approximately 5 μm) were sequentially treated as follows. After deparaffinization and microwave treatment, sections were incubated with the primary antibody for one hour at room

Table 1. Laboratory data in *fa/fa* and *fa/+* rats

	fa/fa rats ($N = 9$)	*fa/+* rats ($N = 4$)
Plasma		
Creatinine *mg/dL*	0.19 ± 0.06	0.38 ± 0.07^{b}
Urea *mg/dL*	44 ± 4.9	46 ± 3.5
Triglycerides *mg/dL*	639 ± 153	112 ± 44^{a}
Cholesterol *mg/dL*	268 ± 32	120 ± 12^{a}
Glucose *mg/dL*	195 ± 43	268 ± 26
Creatinine clearance/body weight		
mL/min/100 g	0.52 ± 0.17	0.51 ± 0.13
Urinary excretion		
Protein *mg/24 h*	335 ± 131	7.4 ± 1.5^{a}
Albumin *mg/24 h*	91 ± 48.7	1 ± 0.5^{a}

Results are shown as ± SD.
[a] $P < 0.001$, [b] $P < 0.0001$

Table 2. Morphometric data

	fa/fa rats	*fa/+* rats
	($N = 9$)	($N = 4$)
Glomerulosclerosis *% glomeruli*	24 ± 4.2	0.9 ± 0.8^{b}
Glomerular damage index	147 ± 15	40 ± 6^{b}
Glomerular volume $10^3\ \mu m^3$	3574 ± 284	2283 ± 135^{b}
	($N = 5$)	($N = 4$)
GBM thickness *μm*	1.496 ± 0.076	1.292 ± 0.138^{a}

Results are shown as ± SD.
[a] $P < 0.05$, [b] $P < 0.001$

temperature and were immunostained with Cy 2-labeled anti-rabbit IgG antibodies. For all studies, negative controls were performed with substitution of the primary antibodies with PBS, normal serum, or blocking solution.

Cytochemical techniques

For identification of lipids by LM, 7 μm sections of 2% paraformaldehyde-fixed, paraffin-embedded renal tissue of *fa/fa* obese Zucker rats and controls were stained with oil red according to Lillie [18]. For identification of lipids in TEM, a further *fa/fa* rat tissue was fixed by perfusion with a 1.5% glutaraldehyde solution. Renal cortical tissue was postfixed in a 2% OsO_4, 0.1 mol/L imidazole solution for one hour; according to Angermüller and Fahimi, lipids are stained deep black by this treatment [19].

For discrimination of lysosomes, the acid phosphatase activity was tested by a modified cerium technique developed by Robinson and Karnovsky [20]. A further *fa/fa* rat was fixed by perfusion with a 0.5% glutaraldehyde solution. From renal cortical tissue, 100 μm sections were cut with a tissue chopper. After preincubation for 30 minutes in a medium without substrate, the sections were incubated in a medium containing 10 mmol/L cytidine 5′ monophosphate (Sigma, Heidelberg, Germany), 3 mmol/L $CeCl_3$ in 50 mmol/L acetate buffer, pH 5, at 37°C for 60 minutes. Acid phosphatase activity was finally demonstrated by postfixation with reduced osmium containing 1% aqueous OsO_4 and 1.5% potassium ferrocyanide. After dehydration in a graded series of ethanols, the sections were embedded in Epon 812; ultrathin sections were observed by TEM.

Tracer studies

To verify misdirected filtration from segmentally injured glomeruli, tracer studies with ferritin (according to a previously applied protocol [21]) were performed. In healthy kidneys, ferritin is not filtered but, when exogenously administered, passes in small amounts through the GBM and is eventually picked up by endocytosis by podocytes [22]. In injured glomeruli with damage to the filtration barrier, ferritin passes in bulk through a leaky GBM and is subsequently taken up by endocytosis by podocytes or travels with the tubular urine, from where it is (at least partially) reabsorbed by the proximal tubules [23–26].

In the present experiments, a commercial preparation of native horse spleen, that is, anionic ferritin (F-4503; Sigma) containing 100 mg protein/mL was used, carefully prepared as previously described [21]. The solution was slowly administered into the tail vein of two anesthetized *fa/fa* rats in a dose of 100 mg ferritin per 100 g body weight. In the first animal, the kidneys were removed 30 minutes after the end of ferritin application in the second after 60 minutes. The kidneys were cut into slices fixed by immersion in 4% paraformaldehyde for several hours and embedded into paraffin by standard procedures. Series of 8 μm sections were prepared. Ferritin was visualized in the sections by the potassium ferrocyanide method (Prussian blue reaction) [27]. The sections were counterstained with nuclear fast red and observed by LM.

Statistical analyses

Data are presented as means ± SD. The statistical evaluation was performed by using the Statistical Analysis System (SAS). The following SAS procedures were applied: PROC NPAR1WAY for performing the Kruskal–Wallis test and PROC REG for calculating regression analysis (SAS Institute Inc., Carey, NC, USA).

RESULTS

Pathophysiological data

Body weight differed between *fa/fa* and *fa/+* rats (Table 1). The plasma urea values showed no difference. All *fa/fa* rats exhibited significant hyperlipidemia. Compared with the usual values encountered in rats, plasma glucose levels were increased in both groups, probably because of the anesthesia. The *fa/fa* rats exhibited pronounced proteinuria and albuminuria as compared with their controls.

Morphometric analyses revealed significantly larger glomerular volumes in the *fa/fa* rats as compared with *fa/+* animals (Table 2). The same was true for the per-

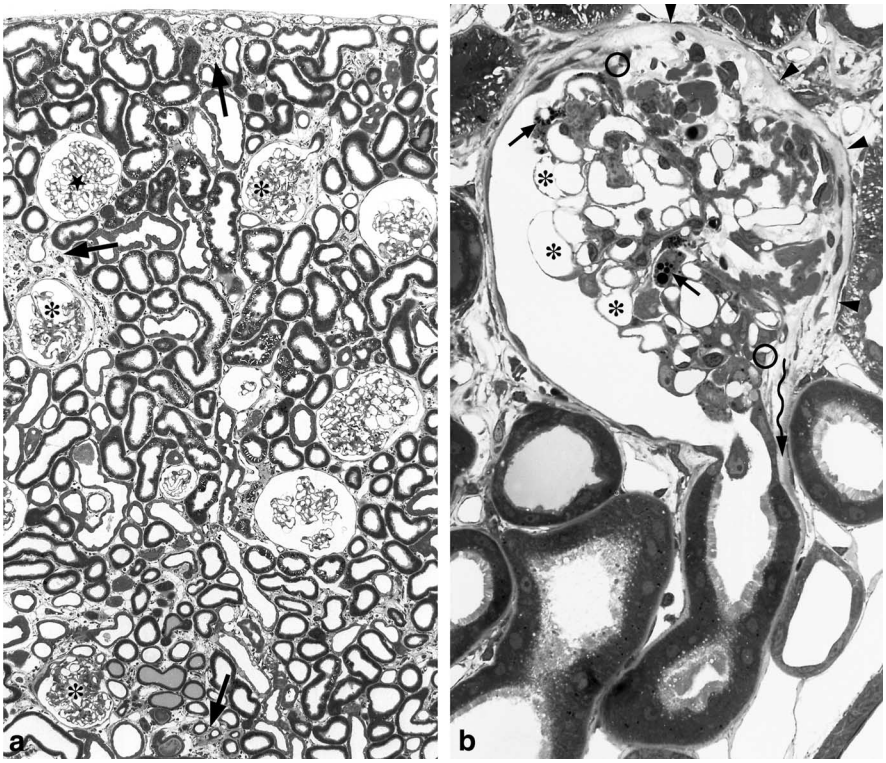

Fig. 1. (*a*) Overview of renal cortex displaying glomerular profiles in different stages of sclerosis development (asterisks); glomerular profiles of normal appearance are also seen (stars). Foci of tubular degeneration and interstitial proliferation are found (arrows). (*b*) Segmental glomerular injury with adhesion to Bowman's capsule, formation of a paraglomerular space, delimitation of this space toward the interstitium by a barrier of fibroblasts (arrowheads), and extension of the paraglomerular space—via the urinary pole—onto the outer aspect of the proximal tubule (serpentine arrow). Note the large gap in the parietal epithelium (between the two circles that label the two terminations of the parietal epithelium) through which the "sclerotic" tuft portion is herniated into the paraglomerular space. Also, the "intact" tuft portion (which protrudes into Bowman's space) displays severe podocyte injury, including foot process effacement, pseudocyst formation (asterisks), and accumulation of absorption droplets (arrows). (a) *fa*/*fa* Zucker rat, 10 months, LM ×~60; (b) *fa*/*fa* Zucker rat, 10 months, LM ×~340.

centage of sclerosed glomeruli and the damage index. In the *fa*/*fa* rats, mean glomerular and tuft volume correlated with proteinuria ($r = 0.6070$, $r = 0.6285$) and albuminuria ($r = 0.5918$, $r = 0.6041$).

Histopathology

As shown by the damage index and by the frequency of glomerulosclerosis, the degree of renal damage was similar among individual rats. Throughout the renal cortex, the characteristic picture of "classic" FSGS was seen; various stages of tuft adhesions and fully developed synechiae were encountered. Associated with injured glomeruli were changes in the tubulointerstitium consisting of tubular ectasia, atrophy, and obstruction accompanied by interstitial fibrosis (Fig. 1a).

Approximately a quarter of the glomeruli exhibited sclerotic lesions (Table 2), and generally the adhesion-mediated type of glomerulosclerosis was obvious (Fig. 1b). In addition, extensive "presclerotic" lesions were prominent. This was likewise found in glomeruli without an already established adhesion and in nonsclerotic portions of glomeruli with established adhesions. Their features included changes in tuft architecture, notably capillary ballooning as well as cellular injuries of podocytes, among them foot process effacement, cell body attenuation, and extensive pseudocyst formation (Figs. 1b and 2a). Quite typically, podocytes that contained accumulations of cytoplasmic granules of different electron densities were encountered. By specific LM and TEM techniques, it could be shown that at least part of them were lipid droplets and others were lysosomes (Fig. 2). Lipid droplets were also seen in mesangial cells. By morphometry at the TEM level, a significant increase in GBM thickness compared with controls was found (Table 2).

The tuft adhesions to Bowman's capsule exhibited the typical structural features known from other rat models of "classic" adhesion-mediated FSGS (Figs. 1 and 3) [28–31]. The sclerotic tuft portion associated with an adhesion consisted of podocyte-deprived hyalinized or collapsed capillary remnants essentially made up of wrinkled layers of former GBM (Fig. 1b). Generally, these sclerotic tuft portions had come to lie outside of the parietal epithelium enclosed within paraglomerular spaces. Toward the interstitium, the paraglomerular spaces were delimited by a layer of fibroblasts/fibroblast processes. Important to note and clearly seen in Figure 3a, those degenerating tuft portions contained—in addition to collapsed and hyalinized capillaries—patent capillaries that were obviously perfused.

In advanced stages of this degenerative process, the paraglomerular spaces, via the urinary pole, extended onto the corresponding proximal tubule by separating the tubular basement membrane (TBM) from its epithe-

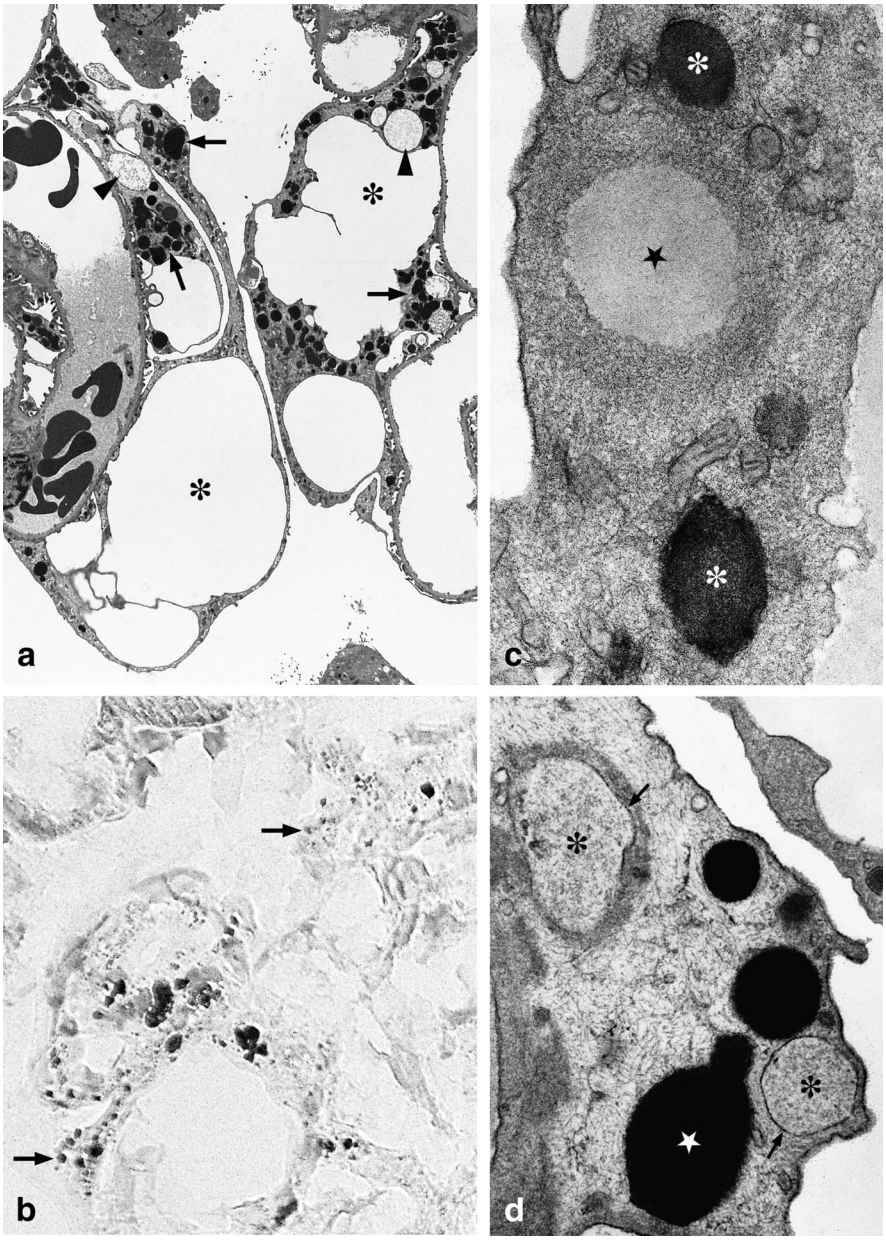

Fig. 2. Lesions encountered in podocytes. (*a*) In addition to foot process effacement (not very prominent in this case) and pseudocyst formation (asterisks), podocytes frequently contain cytoplasmic inclusions of different electron densities. After routine staining techniques, many of them show up in deep black (arrows), whereas others are much less electron dense (arrowheads). (*b*) Staining with oil red identifies lipid accumulations in podocytes [arrows; black stained inclusions; the original red color has been (intensity corrected) converted into black]; similar accumulations are seen in mesangial regions. (*c*) Activity for acid phosphatase identifies a group of cytoplasmic inclusions as lysosomes (asterisks). Others were non-reactive, suggesting that they are lipid droplets (star) supported by the lack of a limiting membrane. (*d*) Positive staining with a cerium phosphate reaction identifies lipid inclusions (star). Unstained inclusions (asterisks) are clearly bordered by a membrane (arrows), suggesting that they are lysosomes. *fa/fa* Zucker rat, 10 months (a) TEM ×~1500; (b) LM ×~650; (c) TEM ×~27,000; (d) TEM ×~22,000.

lium or simply by expanding the TBM (Figs. 1b and 3 a, b). This promoted the formation of subepithelial peritubular fluid filled spaces, which like the corresponding spaces at the glomerulus, became delimited from the interstitium by a layer of fibroblast processes.

In more downstream portions of the proximal tubule, the subepithelial peritubular spaces continued simply by expanding the TBM. As shown by immunocytochemistry (Fig. 4), those thickened cylinders of TBM exclusively consisted of collagen type IV, not of collagen type I, excluding that these peritubular matrix cylinders had been produced by the fibroblasts by which they were surrounded. Later, associated with the collapse and atrophy of the epithelial tubes, further spaces developed between the expanded TBM and the epithelial cords (Figs. 3 c–e and 5). Finally, the epithelial remnants fully disappeared leaving behind empty (that is, fluid filled) wrinkled cylinders of former TBM.

As seen in Figure 5, the degenerative process was strictly focal in nature and confined to the affected nephron. None of the adjacent nephrons, neither glomeruli nor tubules, appeared to be seriously attacked by the pathologic process in their surroundings. By tracing in serial sections, it became obvious that tubular coils of healthy nephrons, even if fully surrounded by degenerating tubules, preserve the usual features of a differentiated epithelium (Fig. 5).

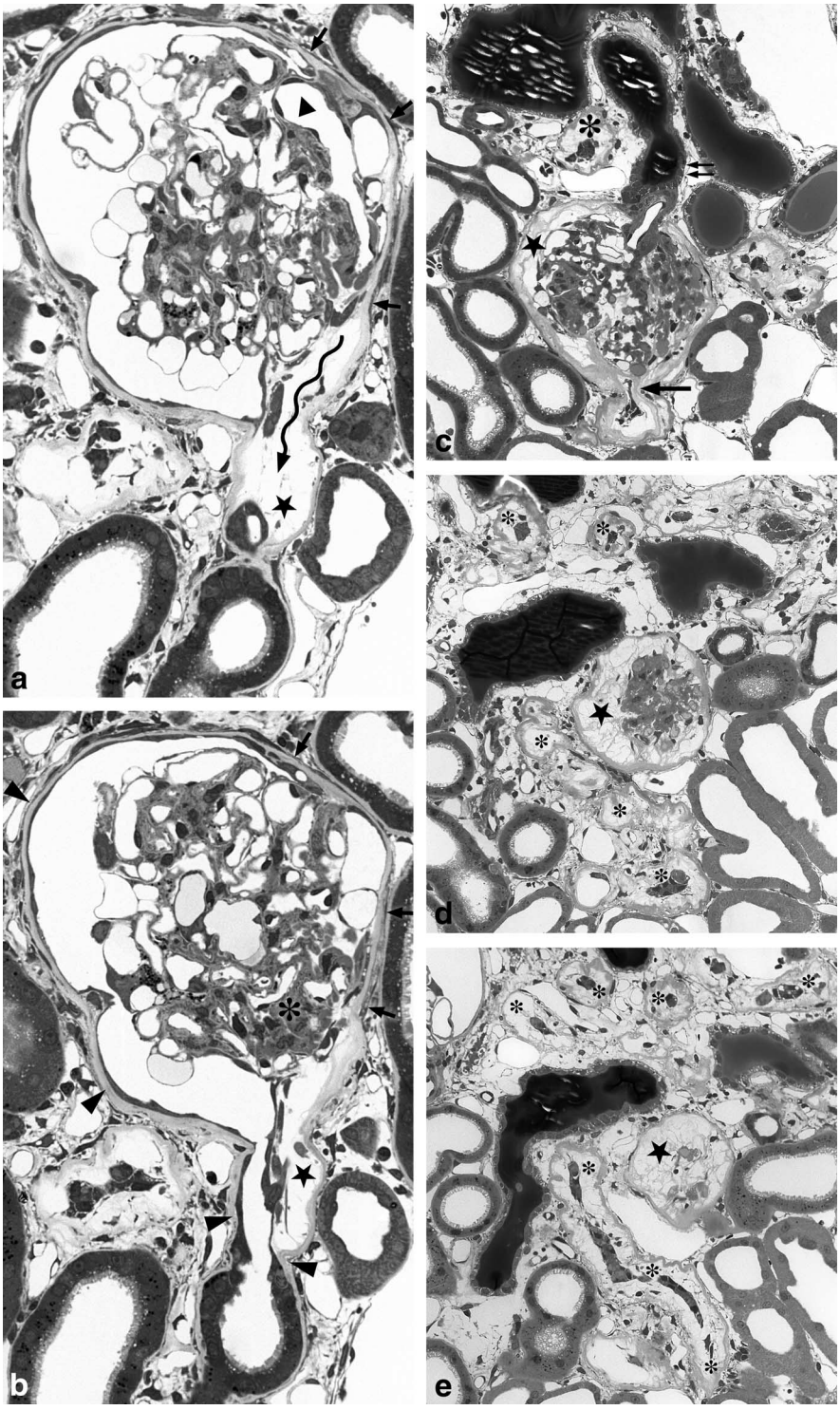

Fig. 3. Degeneration of glomerulus and corresponding tubule are associated with each other. (*a* and *b*) Two subsequent sections through the glomerulotubular junction of a glomerulus with segmental glomerulosclerosis. The "sclerotic" tuft portion (asterisk) adheres to the Bowman's capsule, being associated with a prominent paraglomerular space that is delimited from the interstitium by a layer of fibroblasts (small arrows). At the urinary pole, this space extends to the outer aspect of the corresponding tubule (serpentine arrow). The initial segment of the tubule consists of a thin epithelium surrounded by wide subepithelial peritubular spaces (stars) that obviously have developed between the epithelium and its basement membrane. More distally, as well as on the opposite side of the tubule, the spaces continue as a much expanded basement membrane (arrowheads). Also, the periglomerular basement membrane is expanded (arrowhead) throughout the glomerular circumference. Note that the sclerotic tuft portion that adheres to Bowman's capsule contains a patent capillary (triangle). (*c–e*) Consecutive sections of a severely injured nephron showing the continuation between the glomerular and the tubular injury. A "sclerotic" and collapsed glomerular tuft is enclosed by a prominent paraglomerular space (star) that (at the glomerulotubular junction) extends to the outer aspect of the tubular remnant (large arrow). These peritubular spaces accompany the remains of the tubule consisting of a solid cord of cells. All tubular remnants (asterisks) surrounded by such spaces seen in this picture belong to the same nephron (traced serial sections). There is considerable enlargement of the interstitial space surrounding the tubular remnants. Note that in the vicinity of such severely damaged tubules tubular profiles from other nephrons are encountered that look perfectly intact. Corresponding distal tubules (identified by the contact of the macula densa to the glomerular vascular pole; two small arrows) are filled with proteinaceous material. *fa/fa* Zucker rat; 10 months (a) LM × ~330; (b) LM × ~330; (c) LM × ~180; (d) LM × ~180; (e) LM × ~180.

Tracer studies with ferritin

The observations concerning the distribution of exogenously administered ferritin in injured nephrons fully agreed with what had been seen recently in similar experiments in other genetic models of FSGS [21]. In contrast to healthy nephrons (data not shown), in injured nephrons, ferritin was seen to escape from glomerular capillaries and to leak into tuft adhesions, becoming densely accumulated in regions of hyalinosis (Fig. 6). In addition, within paraglomerular spaces, as well as within the expanded basement membrane of the parietal epithelium (PBM), ferritin had spread around the entire circumfer-

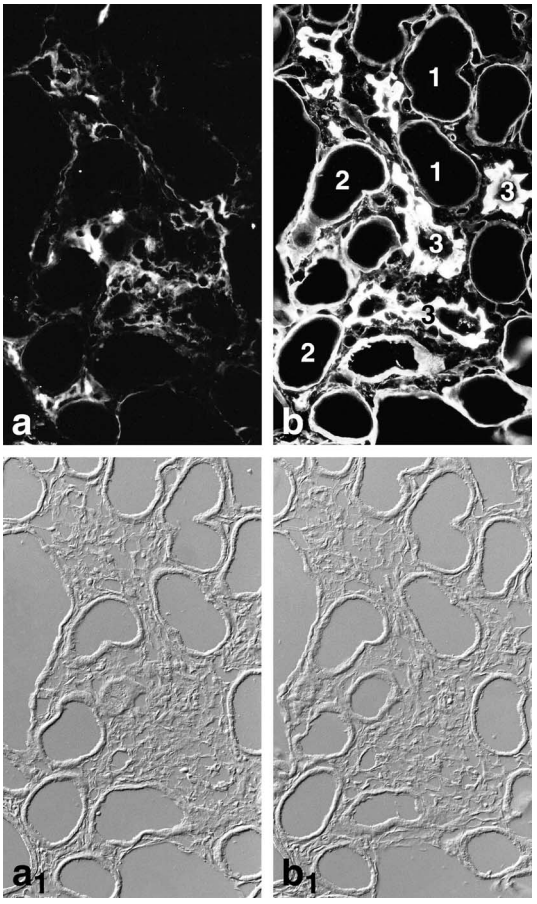

Fig. 4. Composition of the matrix that surrounds degenerating tubules analyzed by immunofluorescence of serial sections; a_1 and b_1 show the corresponding sections by phase contrast microscopy. (*a*) Collagen type I is exclusively found outside the prominent subepithelial peritubular matrix spaces that surround the degenerating tubules. (*b*) The subepithelial peritubular spaces contain abundant collagen type IV. Three types of tubular profiles are seen. Those labeled with (*1*) are obviously healthy tubules exhibiting a thin basement membrane; labeled with (*2*) are patent tubules surrounded by expanded basement membranes; those labeled with (*3*) are collapsed tubules with wrinkled peritubular matrix cylinders representing the former TBM. *fa/fa* Zucker rat; 10 months, LM ×~120.

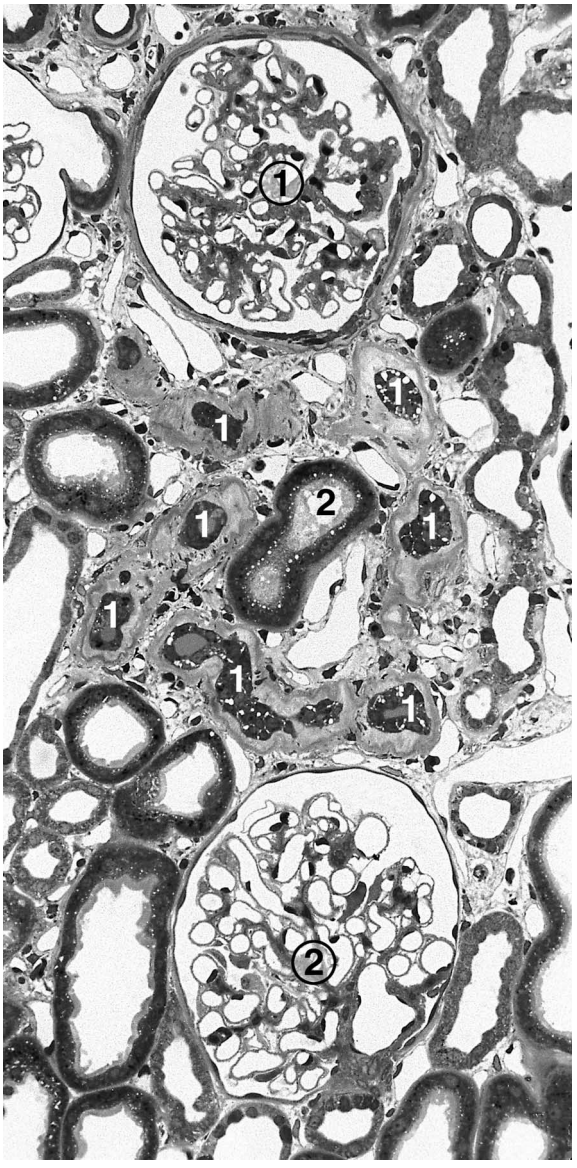

Fig. 5. Tubular degeneration as traced in serial sections. The injured glomerulus labeled with 1 exhibits segmental glomerulosclerosis with a broad synechia (not seen in this particular section). All tubular profiles labeled with 1 belong to this glomerulus. They all are collapsed and contain epithelial remnants surrounded by prominent subepithelial spaces that consist of the expanded former TBM and, in addition, of less electron-dense spaces between the TBM and the epithelial remnant. The glomerulus labeled with 2 is apparently intact (verified in serial sections). One of the profiles that belongs to this glomerulus (labeled with 2) is totally surrounded by the degenerating tubules of glomerulus 1. Note the vivid interstitial proliferation surrounding the injured tubules; the intact profile is enclosed by this interstitial reaction. *fa/fa* Zucker rat; 10 months, LM ×~250.

ence of an affected glomerulus. Toward the interstitium, the blue-stained PBM was sharply delimited; healthy glomeruli never showed such a periglomerular staining, excluding the possibility that the protein had reached this site from the interstitium.

In severely damaged nephrons, the periglomerular ferritin accumulation extended alongside the glomerulotubular junction onto the outer aspect of the proximal tubule and continued for variable distances along the tubule (Fig. 6). Frequently, a group of proximal tubular profiles in the vicinity of the affected glomerulus was involved. As documented in serial sections, these profiles all belonged to the same injured nephron. As seen after a second staining of the sections by the trichrome technique (data not shown), the ferritin stained regions represented subepithelial peritubular spaces that, as documented by TEM, were separated from the interstitium proper by a layer of fibroblast processes. A more in-depth analysis of ferritin distribution in injured nephrons in similar experiments in other models of FSGS has been presented recently [21].

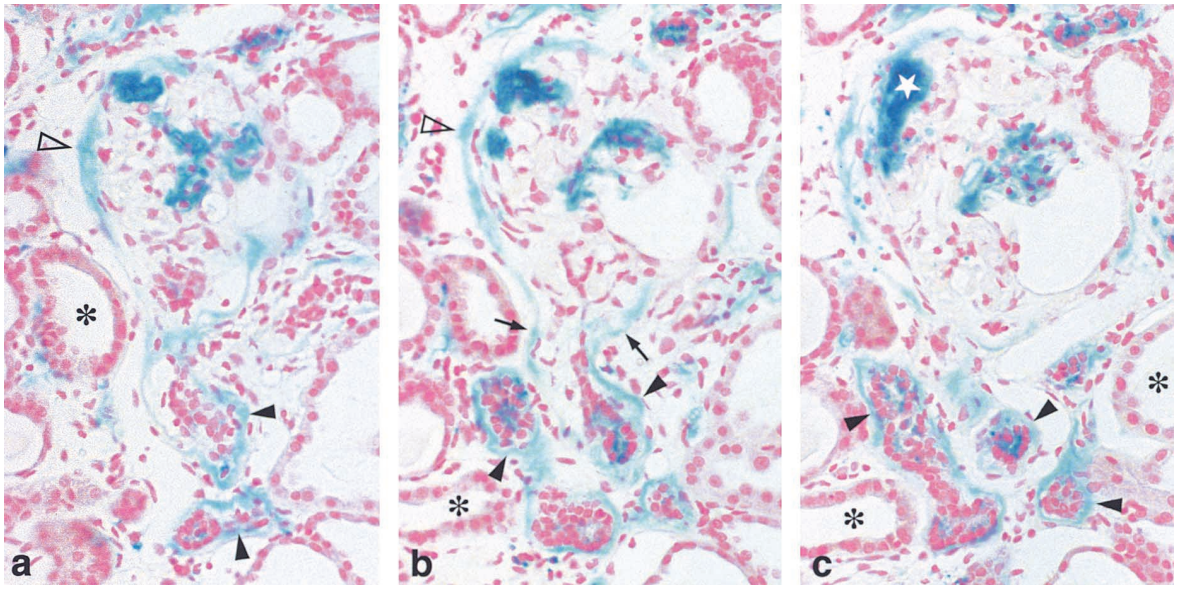

Fig. 6. Renal cortex of a *fa/fa* Zucker rat 60 minutes after the application of ferritin and its subsequent visualization by the potassium ferrocyanide method in three consecutive sections (*a–c*). In contrast to controls (data not shown), in injured nephrons, ferritin is accumulated within the sclerotic tuft portions, especially in areas with hyalinosis (star); second, ferritin stains the expanded parietal basement membrane that is sharply delimited toward the interstitium (open arrowheads); third, at the glomerulotubular junction, the staining extends onto the outer aspect of the degenerated and obviously obstructed tubule (arrows). The damaged tubular profiles are all surrounded by blue staining collars (arrowheads). Intact tubules (asterisks) do not show any peritubular ferritin accumulation. *fa/fa* Zucker rat; 10 months, Prussian blue reaction and nuclear fast red counter staining, LM ×~250.

DISCUSSION

Obese *fa/fa* Zucker rats are considered as a model for the metabolic syndrome associated with non-insulin–dependent diabetes mellitus and obesity [5–9, 32–34]. This view is supported by the high plasma triglyceride as well as cholesterol levels, glomerular hypertrophy, and glomerular hyperfiltration found in the present study. A recent study about the nephropathy encountered in these animals by Coimbra et al focused on the early renal changes in this disease [9]; the present study started at later stages to analyze the manner in which a nephron degenerates. Both studies are in perfect agreement in the finding that the glomerular disease starts with podocyte injury.

The first goal of this study was to elucidate the sequence of histopathological events leading from podocyte injury to glomerulosclerosis and further on to the degeneration of the entire nephron. Not surprisingly, the histopathology encountered in this model is quite similar to what was seen in other nondiabetic rat models of nephron degeneration [29, 30, 35, 36]. The glomerular lesions were focally distributed and were of the "classic-type" FSGS. Early structural damage of podocytes consisted in foot process effacement, cell body attenuation, as well as pseudocyst formation frequently associated with cytoplasmic accumulation of lipid droplets and lysosomal elements.

Later stages of injury consisted in the formation of tuft adhesions to Bowman's capsule. Like in other rat models of FSGS, the "sclerotic" tuft portions were herniated through gaps in Bowman's capsule out into paraglomerular spaces. As shown in previous work, the development of those spaces was dependent on misdirected filtration toward the interstitium out of perfused capillaries contained in the adhesion [21, 29, 35, 37]. Misdirected filtration was verified also in the present model. Tracer experiments with ferritin clearly showed the exit of the tracer from glomerular capillaries into the adhesion and, further on, around the outer aspect of the glomerulus as well as via the glomerulotubular junction, onto the outer aspect of the corresponding tubule. Thus, the nephron degeneration in this model of diabetic nephropathy followed a nonspecific pathway, which is common to a variety of rat models of classic, adhesion-mediated FSGS [28, 35].

This observation raises the question as to what extent the lesions seen in this model mimic the lesions encountered in diabetic nephropathy in humans. Thus, is it appropriate to consider this rat as a model for the nephropathy seen in type II diabetes in humans. No question, if we consider the early lesions in humans, that is, mesangial expansion and matrix deposition [38, 39], there is little correspondence between the rat model and the human disease. In agreement with the already mentioned recent study [9], we found little mesangial damage and/or mesangial expansion in nonsclerotic glomeruli in this rat

model. Thus, it is obvious that the long-lasting period in human cases of diabetic nephropathy with its slowly increasing amounts of mesangial matrix accumulation is missing in this model [39, 40].

However, the histopathological changes encountered in later stages of the disease are quite similar. Also, in human cases, the segmental glomerular injury of diabetic nephropathy is of the classic FSGS type [35], with formation of glomerular synechia [41] and extension of the damage along the outside of the urinary pole onto the corresponding tubule [35]. Dilated or atrophic tubular profiles surrounded by a tremendously thickened basement membrane and/or peritubular spaces are typically encountered in human cases of diabetic nephropathy as well [42, 43]. Such peritubular matrix cylinders have generally been interpreted as an additional (that is, additional to the mesangium) locus of matrix deposition by adjacent cells (epithelial cells, fibroblasts) [41]. In the *fa*/*fa* rat, there is no mesangial expansion with matrix deposition. Nevertheless, voluminous matrix-filled spaces around atrophic or degenerating tubules are regularly observed. The present investigation provides strong evidence (as did previous studies of other models in the rat [21, 35]) that the formation of these peritubular spaces is initiated by subepithelial peritubular filtrate spreading. Additional strong evidence in favor of this assumption is provided by our immunocytochemical observations. The matrix cylinders around the degenerating tubules exclusively contain collagen type IV, which is known to be produced in increasing amounts by proximal tubules under high ambient glucose conditions [44–47].

There is evidence that the development of such fluid/matrix-filled subepithelial peritubular spaces occurs in a similar manner in humans [35, 42, 43]. In biopsies from patients with diabetic nephropathy, it was previously documented that plasma borne compounds (albumin, unspecific IgG) may accumulate in glomerular synechiae as well as peritubular cylinders around degenerating tubules [48, 49]. Even the continuity between the paraglomerular and the peritubular staining at the glomerulotubular junction was shown [48], suggesting that these substances have reached the tubule by misdirected filtration and peritubular filtrate spreading. Taken together, the obese *fa*/*fa* Zucker rats do not appear to represent a model for the mesangial changes (including the formation of nodules) seen in human diabetic nephropathy, but they probably correctly mimic the more advanced lesions actually leading to the degeneration of the nephron.

The second main question of our study deals with the mechanisms underlying the progression of the disease once it is established. The foundation of the progression of chronic renal failure is the progressive loss of viable nephrons. In addition to the possibility that each nephron is separately affected by the same systemic or glomerular factors, at present, a widely favored hypothesis is that there is a nephron-to-nephron transfer of the disease at the level of the tubulointerstitium. Although the disease starts at the glomerulus, local tubulointerstitial mechanisms, notably interstitial proliferation and matrix deposition, are thought to become the dominating processes leading to progressive renal scarring followed by the loss of further nephrons. The most frequently discussed concept as to how the injury that originates in the glomerulus spreads to the tubulointerstitium suggests that glomerular protein leakage represents the decisive link between glomerular and tubulointerstitial injury [50–52]. An injured filtration barrier allows excessive leakage of plasma proteins into the tubular urine, followed by the reabsorption of these proteins by proximal tubules. In response, the tubules secrete mediators (such as monocyte chemokine protein type I, platelet-derived growth factor, osteopontin, endothelin, and others) toward the interstitium, giving rise to interstitial proliferation and matrix deposition. These interstitial processes subsequently are considered to account (*1*) for the final destruction of the already affected nephron and (*2*) for the transfer of the disease to neighboring nephrons with the destructive processes now starting at the tubule [51–54].

Our present study does not provide evidence for such a mechanism. There are generally sharp borders between degenerating and healthy tubular profiles. In the immediate vicinity or even amidst groups of degenerating tubules, tubular profiles are found that are structurally fully intact. When followed in serial sections, it can clearly be shown that they belong to a neighboring healthy nephron. Moreover, no specific histopathological changes were encountered, suggesting that a sequence of pathological events has led to the degeneration of nephrons different from the usual one. This is in full agreement with previous work demonstrating that the manner in which the nephron undergoes destruction along with misdirected filtration and peritubular filtrate spreading assures that the destructive effects remain confined to the initially affected nephron [21, 35].

The same sharp borders between affected and healthy nephrons are also seen in kidneys from human cases of diabetic nephropathy (personal observations) [42]. Thus, neither in animal models nor in human cases is there structural evidence that the disease, via interstitial proliferation, jumps from the affected nephron to another as yet unaffected nephron. In contrast, the focal distribution among nephrons (clearly seen in early stages of the disease) represents strong evidence that the destructive process starts separately in each nephron. Interstitial proliferation as it locally occurs in the surroundings of injured tubules and glomeruli apparently develops secondary to tubular degeneration, and finally replaces a deadly injured nephron but does not appear to be harmful to a neighboring unaffected nephron.

In conclusion, there is obviously no particular tubulointerstitial driving force for disease progression. This brings us back to the question of determining the damaging factors leading to early podocyte disease in this model. Thus far, there is no evidence that high glucose levels are directly toxic to podocytes; however, there are several indications that podocytes—far in advance of any structural injuries—respond to hyperglycemia with changes in cell metabolism [55–58]. The relevance of the changes in intermediate filament expression from vimentin towards desmin is unknown; however, it represents a consistent symptom associated with increased challenges to podocytes under a variety of circumstances [36, 59, 60]. The increased leakiness of the filtration barrier leading to the most early symptom in diabetic patients to albuminuria can readily be expected to be podocyte dependent. Podocytes are largely responsible for the turnover of the GBM, and there is general agreement that the changes in GBM thickness ([61]; also seen in the *fa*/*fa* Zucker rat in a previous [9] and the present study) and GBM composition (loss of anionic charges in the GBM due to undersulfated glycosaminoglycan side chains of heparan sulfate proteogylcans) already encountered at early stages of diabetic nephropathy [62] account for the loss of permselectivity. We hypothesize that this increased leakage of the GBM for macromolecules is a major factor for the initial podocyte damage as well as for damage progression. As part of their GBM cleaning function, podocytes take up a great variety of macromolecules by endocytosis in order to convey them to lysosomal degradation. It appears that podocytes have a limited capacity for this function. Podocytes filled with absorption droplets and other lysosomal elements, including lipid droplets, are a consistent observation in the present and previous studies [60, 63]. Such an overload in lysosomal degradation possibly exposes podocytes to the danger of spillage of lysosomal enzymes into the cytoplasm, leading to severe injury and finally to cell death (as has been recently suggested for the proximal tubule [52]). Thus, there may well be some kind of an intraglomerular vicious circle starting with podocyte insufficiency leading to increased leakage of macromolecules through the GBM, a process that in turn increases podocyte damage. Supportive of such a mechanism are recent studies showing that the effects of ACE inhibition leading to a decrease in protein excretion and deceleration in disease progression (as seen in several studies [53, 64, 65]) actually occur in the podocyte [37].

Taken together, according to what is encountered structurally, the disease always starts separately in each nephron in the glomerulus. If there are no other aggressive pathogenetic factors (for example, glomerular hypertension), a slowly increasing defect in permselectivity of the glomerular filter may be the chronic damaging mechanism to podocytes that lead to the sequence of events that, via the development of FSGS, finally result in the degeneration of the entire nephron. From this point of view, the driving force for tubulointerstitial injury is a gradual but lasting loss of podocytes, leading to a corresponding loss of nephrons that is replaced by interstitial scar tissue.

ACKNOWLEDGMENTS

The study was carried out with a generous support by the "Gotthard-Schettler-Gesellschaft für Herz-und Kreislaufforschung," Heidelberg. We thank Ingrid Ertel for the photographic work and Rolf Nonnenmacher for the art work.

Reprint requests to Dr. Wilhelm Kriz, Im Neuenheimer Feld 307, Institut für Anatomie und Zellbiologie, Medizinische Fakultät Heidelberg, Universität Heidelberg, D-69120 Heidelberg, Germany.
E-mail: wilhelm.kriz@urz.uni-heidelberg.de

REFERENCES

1. Peterson RG, Shaw WN, Neel MA, *et al:* Zucker diabetic fatty rat as a model for non-insulin-dependent diabetes mellitus. *Inst Lab Anim Res* 32:16–19, 1990
2. Kurtz TW, Morris RC, Pershadsingh HA: The Zucker fatty rat as a genetic model of obesity and hypertension. *Hypertension* 13:896–901, 1989
3. Ionescu E, Sauter JF, Jeanrenaud B: Abnormal oral glucose tolerance in genetically obese (fa/fa) rats. *Am J Physiol* 248:500–506, 1985
4. Ogawa Y, Masuzaki H, Isse N, *et al:* Molecular cloning of rat obese cDNA and augmented gene expression in genetically obese Zucker fatty (fa/fa) rats. *J Clin Invest* 96:1647–1652, 1995
5. Zucker LM: Hereditary obesity in the rat associated with hyperlipemia. *Ann NY Acad Sci* 131:447–458, 1965
6. Kasiske BL, O'Donnell MP, Keane WF: The Zucker rat model of obesity, insulin resistance, hyperlipidemia, and renal injury. *Hypertension* 19:110–115, 1992
7. Phillips MS, Liu Q, Hammond HA, *et al:* Leptin receptor missense mutation in the fatty Zucker rat. (letter) *Nat Genet* 13:18–19, 1996
8. Gades MD, Van Goor H, Kaysen GA, *et al:* Brief periods of hyperphagia cause renal injury in the obese Zucker rat. *Kidney Int* 56:1779–1787, 1999
9. Coimbra TM, Janssen U, Gröne H-J, *et al:* Early events leading to renal injury in obese Zucker (fatty) rats with type II diabetes. *Kidney Int* 57:167–182, 2000
10. Vora JP, Zimsen SM, Houghton DC, *et al:* Evolution of metabolic and renal changes in the ZDF/Drt-fa rat model of type II diabetes. *J Am Soc Nephrol* 7:113–117, 1996
11. Kasiske BL, Cleary MP, O'Donnell MP, *et al:* Effects of genetic obesity on renal structure and function in the Zucker rat. *J Lab Clin Med* 106:598–604, 1985
12. Magil AB, Frohlich JJ: Monocytes and macrophages in focal glomerulosclerosis in Zucker rats. *Nephron* 59:131–138, 1991
13. Magil AB: Tubulointerstitial lesions in young Zucker rats. *Am J Kidney Dis* 25:478–485, 1995
14. Lavaud S, Michel O, Sassy-Prigene C, *et al:* Early influx of glomerular macrophages precedes glomerulosclerosis in the obese Zucker rat model. *J Am Soc Nephrol* 7:2604–2615, 1996
15. Kaissling B, Kriz W: Variability of intercellular spaces between macula densa cells: A transmission electron microscopic study in rabbits and rats. *Kidney Int* 22(Suppl 12):S9–S17, 1982
16. Richardson KC, Jarett L, Finke EH: Embedding in epoxy resins for ultrathin sectioning in electron microscopy. *Stain Technol* 35:313–325, 1960
17. Jensen EB, Gundersen HJG, Osterby R: Determination of membrane thickness distribution from orthogonal intercepts. *J Microsc* 115:19–33, 1979
18. Lillie RD: Various oil soluble dyes as fat stains in the supersaturated isopropanol technic. *Stain Technol* 19:55–58, 1944

19. Angermüller S, Fahimi HD: Imidazole-buffered osmium tetroxide: An excellent stain for visualization of lipids in transmission electron microscopy. *Histochem J* 14:823–835, 1982
20. Robinson JM, Karnovsky MJ: Ultrastructural localization of several phosphatases with cerium. *J Histochem Cytochem* 31:1197–1208, 1983
21. Kriz W, Hartmann I, Hosser H, *et al:* Tracer studies in the rat demonstrate misdirected filtration and peritubular filtrate spreading in with segmental glomerulosclerosis. *J Am Soc Nephrol* 12: 496–506, 2001
22. Farquhar MG, Wissig SL, Palade GE: Glomerular permeability. I. Ferritin transfer across the normal glomerular capillary wall. *J Exp Med* 113:47–66, 1961
23. Farquhar MG, Palade GE: Glomerular permeability. II. Ferritin transfer across the glomerular capillary wall in nephrotic rats. *J Exp Med* 114:699–715, 1961
24. Kanwar YS, Rosenzweig LJ, Kerjaschki D: Glycosaminoglycans of the glomerular basement membrane in normal and nephrotic states. *Renal Physiol* 4:121–130, 1981
25. Bliss DJ, Brewer DB: Ultrastructural localization of anionic and cationic ferritin in the rat glomerular basement membrane in protein-overload proteinuria. *J Pathol* 143:57–68, 1984
26. Maunsbach AB: Absorption of ferritin by rat kidney proximal tubule cells. *J Ultrastruct Res* 16:1–12, 1966
27. Perls M: Prussian blue technique/Berlinerblau Reaktion, in *Romeis: Mikroskopische Technik* (vol 1, 17th ed), edited by Böck P, München, Wien, Baltimore, Urban und Schwarzenberg, 1989, pp 564–564
28. Kriz W, Lemley KV: The role of the podocyte in glomerulosclerosis. *Curr Opin Nephrol Hypertens* 8:489–497, 1999
29. Kriz W, Hosser H, Hähnel B, *et al:* Development of vascular pole associated glomerulosclerosis in the Fawn-hooded rat. *J Am Soc Nephrol* 9:381–396, 1998
30. Shirato I, Hosser H, Kimura K, *et al:* The development of focal segmental glomerulosclerosis in Masugi nephritis is based on progressive podocyte damage. *Virchows Arch* 429:255–273, 1996
31. Kretzler M, Koeppen-Hagemann I, Kriz W: Podocyte damage is a critical step in the development of glomerulosclerosis in the uninephrectomized desoxycorticosterone rat. *Virchows Arch A Path Anat Histol* 425:181–193, 1994
32. Kasiske BL, O'Donnell MP, Leary MP, *et al:* Treatment of hyperlipidemia reduces glomerular injury in obese Zucker rats. *Kidney Int* 33:667–672, 1988
33. Schmitz PG, O'Donnell MP, Kasiske BL, *et al:* Renal injury in obese Zucker rats: Glomerular hemodynamic alterations and effects of enalapril. *Am J Physiol* 263:F496–F502, 1992
34. Yoshioka S, Nishino H, Shiraki T, *et al:* Antihypertensive effects of CS-045 treatment in obese Zucker rats. *Nephron* 59:131–138, 1991
35. Kriz W, Hosser H, Hähnel B, *et al:* From segmental glomerulosclerosis to total nephron degeneration and interstitial fibrosis: A histopathological study in rat models and human glomerulopathies. *Nephrol Dial Transplant* 13:2781–2798, 1998
36. Floege J, Hackmann B, Kliem V, *et al:* Age-related glomerulosclerosis and interstitial fibrosis in Milan normotensive rats: A podocyte disease. *Kidney Int* 51:230–243, 1997
37. Macconi D, Ghilardi M, Bonassi ME, *et al:* Effect of angiotensin-converting enzyme inhibition on glomerular basement membrane permeability and distribution of zonula occludens-1 in MWF rats. *J Am Soc Nephrol* 11:477–489, 2000
38. Osterby R: Early phases in the development of diabetic glomerulopathy: A quantitative electron microscopic study. *Acta Med Scand* Suppl 574:3–82, 1974
39. Osterby R, Gundersen HJ, Horlyck A, *et al:* Diabetic glomerulopathy: Structural characteristics of the early and advanced stages. *Diabetes* 32:79–82, 1983
40. Olgemöller B, Schleicher E: Alterations of glomerular matrix proteins in the pathogenesis of diabetic nephropathy. *Clin Invest* 71(Suppl):S13–S19, 1993
41. Olson JL: Diabetes mellitus, in *Pathology of the Kidney* (vol 4, 4th ed), edited by Heptinstall RH, Boston, Little, Brown, 1992, pp 1715–1763
42. Ziyadeh FN, Goldfarb S: The diabetic renal tubulointerstitium. *Curr Top Pathol* 88:175–201, 1995
43. Dodd S: The pathogenesis of tubulointerstitial disease and mechanisms of fibrosis. *Curr Top Pathol* 88:51–67, 1995
44. Ihm CG, Lee GSL, Nast CC, *et al:* Early increased renal procollagen α1 (IV) mRNA levels in streptozotocin induced diabetes. *Kidney Int* 41:768–777, 1992
45. Ziyadeh FN: Renal tubular basement membrane and collagen type IV in diabetes mellitus. *Kidney Int* 43:114–120, 1993
46. Bleyer AJ, Fumo P, Snipes ER, *et al:* Polyol pathway mediates high glucose-induced collagen synthesis in proximal tubule. *Kidney Int* 45:659–666, 1994
47. Han DC, Isono M, Hoffman BB, *et al:* High glucose stimulates proliferation and collagen type I synthesis in renal corical fibroblasts: Mediation by autocrine activation of TGF-β. *J Am Soc Nephrol* 10:1891–1899, 1999
48. Miller K, Michael AF: Immunopathology of renal extracellular membranes in diabetes mellitus: Specificity of tubular basement membrane immunofluorescence. *Diabetes* 25:701–708, 1976
49. Tisher CC, McCoy RC: Diabetes mellitus and the kidney, in *The Kidney in Systemic Disease* (vol 1, 2nd ed), edited by Suki WN, Eknoyan G, New York, John Wiley and Sons, 1981, pp 479–506
50. Abbate M, Zoja C, Corna D, *et al:* In progressive nephropathies, overload of tubular cells with filtered proteins translates glomerular permeability dysfunction into cellular signals of interstitial inflammation. *J Am Soc Nephrol* 9:1213–1224, 1998
51. Burton C, Harris KPG: The role of proteinuria in the progression of chronic renal failure. *Am J Kidney Dis* 27:765–775, 1996
52. Remuzzi G, Bertani T: Pathophysiology of progressive nephropathies. *N Engl J Med* 339:1448–1456, 1998
53. Abbate M, Zoja C, Rottoli D, *et al:* Antiproteinuric therapy while preventing the abnormal protein traffic in proximal tubule abrogates protein- and complement-dependent interstitial inflammation in experimental renal disease. *J Am Soc Nephrol* 10:804–813, 1999
54. Gandhi M, Olson JL, Meyer TW: Contribution of tubular injury to loss of remnant kidney function. *Kidney Int* 54:1157–1165, 1998
55. Kasinath BS: Effect of insulin on high-glucose medium-induced changes in rat glomerular epithelial cell metabolism of glycoconjugates. *Arch Biochem Biophys* 318:286–294, 1994
56. Kasinath BS, Block JA, Singh AK, *et al:* Regulation of rat glomerular epithelial cell proteoglycans by high-glucose medium. *Arch Biochem Biophys* 309:149–159, 1994
57. Pagtalunan ME, Miller PL, Jumping-Eagle S, *et al:* Podocyte loss and progressive glomerular injury in type II diabetes. *J Clin Invest* 99:342–348, 1997
58. van Det NF, van den Born J, Tamsma JT, *et al:* Effects of high glucose on the production of heparan sulfate proteoglycan by mesangial and epithelial cells. *Kidney Int* 49:1079–1089, 1996
59. Floege J, Kriz W, Schulze M, *et al:* Basic fibroblast growth factor augments podocyte injury and induces glomerulosclerosis in rats with experimental membranous nephropathy. *J Clin Invest* 96:2809–2819, 1995
60. Joles JA, Kunter U, Janssen U, *et al:* Early mechanisms of renal injury in hypercholesterolemic or hypertriglyceridemic rats. *J Am Soc Nephrol* 11:669–683, 2000
61. Osterby R, Parving H-H, Hommel E, *et al:* Glomerular structure and function in diabetic nephropathy. *Diabetes* 39:1057–1063, 1990
62. Gambaro G, van der Woude FJ: Glycosaminoglycans: Use in treatment of diabetic nephropathy. *J Am Soc Nephrol* 11:352–368, 2000
63. Gröne H-J, Walli A, Gröne E, *et al:* Induction of glomerulosclerosis by dietary lipids. *Lab Invest* 60:433–441, 1989
64. Gandhi M, Meyer TW, Brooks DP: Effects of eprosartan on glomerular injury in rats with reduced renal mass. *Pharmacology* 59:89–94, 1999
65. Remuzzi A, Fassi A, Bertani T, *et al:* ACE inhibition induces regression of proteinuria and halts progression of renal damage in a genetic model of progressive nephropathy. *Am J Kidney Dis* 34:626–632, 1999